AFRL-RZ-WP-TP-2008-2174

INITIAL CHARACTERIZATION OF THREE-DIMENSIONAL FLOW SEPARATION IN A COMPRESSOR STATOR (PREPRINT)

S. Todd Bailie, Grant A. Hile, and Steven L. Puterbaugh

Fan and Compressor Branch
Turbine Engine Division

JUNE 2008

Approved for public release; distribution unlimited.

See additional restrictions described on inside pages

STINFO COPY

AIR FORCE RESEARCH LABORATORY
PROPULSION DIRECTORATE
WRIGHT-PATTERSON AIR FORCE BASE, OH 45433-7251
AIR FORCE MATERIEL COMMAND
UNITED STATES AIR FORCE

REPORT DOCUMENTATION PAGE	*Form Approved OMB No. 0704-0188*

1. REPORT DATE *(DD-MM-YY)*	2. REPORT TYPE	3. DATES COVERED *(From - To)*
June 2008	Journal Article Preprint	01 June 2006 – 01 June 2008

4. TITLE AND SUBTITLE
INITIAL CHARACTERIZATION OF THREE-DIMENSIONAL FLOW SEPARATION IN A COMPRESSOR STATOR (PREPRINT)

5a. CONTRACT NUMBER
In-house

5b. GRANT NUMBER

5c. PROGRAM ELEMENT NUMBER
62203F

6. AUTHOR(S)
S. Todd Bailie, Grant A. Hile, and Steven L. Puterbaugh

5d. PROJECT NUMBER
3066

5e. TASK NUMBER
04

5f. WORK UNIT NUMBER
306604TK

7. PERFORMING ORGANIZATION NAME(S) AND ADDRESS(ES)
Fan and Compressor Branch (AFRL/RZTF)
Turbine Engine Division
Air Force Research Laboratory, Propulsion Directorate
Wright-Patterson Air Force Base, OH 45433-7251
Air Force Materiel Command, United States Air Force

8. PERFORMING ORGANIZATION REPORT NUMBER
AFRL-RZ-WP-TP-2008-2174

9. SPONSORING/MONITORING AGENCY NAME(S) AND ADDRESS(ES)
Air Force Research Laboratory
Propulsion Directorate
Wright-Patterson Air Force Base, OH 45433-7251
Air Force Materiel Command
United States Air Force

10. SPONSORING/MONITORING AGENCY ACRONYM(S)
AFRL/RZTF

11. SPONSORING/MONITORING AGENCY REPORT NUMBER(S)
AFRL-RZ-WP-TP-2008-2174

12. DISTRIBUTION/AVAILABILITY STATEMENT
Approved for public release; distribution unlimited.

13. SUPPLEMENTARY NOTES
Article submitted to the AIAA. PAO Case Number: WPAFB 08-3869, 27 Jun 2008.
This is a work of the U.S. Government and is not subject to copyright protection in the United States.

14. ABSTRACT
A research program is underway seeking to effect a net decrease in aerodynamic loss of a moderately loaded axial compressor stator passage across varying operating conditions. Three dimensional boundary layer separation, typical at the suction surface corners, can differ greatly from classical two dimensional separation, and is the dominant loss and blockage generating feature in the diffusing flowfield of compressor stators. The initial research phase is presently described, wherein a typical modern stator configuration has been designed, and numerical simulations have been used to characterize the aerodynamic performance and key flow features of the baseline stator configuration. The evaluation has been conducted at the high subsonic inlet Mach design condition as well as off-design conditions, including varying incidence angle and inlet Mach number. Refinement and analysis of the baseline configuration is on-going, but the design's performance suggests it is a typical modern stator, providing a good benchmark for the planned competitive approaches towards performance improvement.

15. SUBJECT TERMS
compressor stator, 3d flow separation, flow control

16. SECURITY CLASSIFICATION OF:			17. LIMITATION OF ABSTRACT:	18. NUMBER OF PAGES	19a. NAME OF RESPONSIBLE PERSON (Monitor)
a. REPORT	b. ABSTRACT	c. THIS PAGE			Steven L. Puterbaugh
Unclassified	Unclassified	Unclassified	SAR	20	19b. TELEPHONE NUMBER *(Include Area Code)* N/A

Standard Form 298 (Rev. 8-98)
Prescribed by ANSI Std. Z39-18

Initial Characterization of Three-Dimensional Flow Separation in a Compressor Stator

S. Todd Bailie,* Grant A. Hile† and Steven L. Puterbaugh‡
Propulsion Directorate
Air Force Research Laboratory
Wright-Patterson AFB,OH,45433

A research program is underway seeking to effect a net decrease in aerodynamic loss of a moderately loaded axial compressor stator passage across varying operating conditions. Three dimensional boundary layer separation, typical at the suction surface corners, can differ greatly from classical two dimensional separation, and is the dominant loss and blockage generating feature in the diffusing flowfield of compressor stators. The initial research phase is presently described, wherein a typical modern stator configuration has been designed, and numerical simulations have been used to characterize the aerodynamic performance and key flow features of the baseline stator configuration. The evaluation has been conducted at the high subsonic inlet Mach design condition as well as off-design conditions, including varying incidence angle and inlet Mach number. Refinement and analysis of the baseline configuration is on-going, but the design's performance suggests it is a typical modern stator, providing a good benchmark for the planned competitive approaches towards performance improvement.

I. Introduction

THREE dimensional boundary layers are characterized by low momentum, near-wall fluid that experiences significant streamwise and cross-flow velocities and velocity gradients. Separation of such boundary layers can be significantly different than classical two dimensional boundary layer separation. Three dimensional boundary layer separation can occur without reversed or stagnated flow and the structure of the flow field is quite complex. For example, vortices form where the flow lifts from the surface. The vortex may then be advected downstream or curve back and form a reattachment point depending on flow conditions.

Three dimensional boundary layers are typical of flow fields existing in the corners of walls coming together approximately normally in the streamwise direction in which there is a cross flow pressure gradient. The cross flow pressure gradient provides the mechanism to induce flow normal to the direction of the main flow, that is, secondary flow. In a compressor stator passage, basically a curved diffuser, such a gradient exists to support the curvature of the main flow field. If the diffuser is imagined as a passage bounded by curved, diverging walls that are capped, top and bottom, by flat walls, the secondary flow is established on the flat walls in a direction away from the concave wall and toward the convex wall. As the flat wall is approached from the mid stream, the streamwise velocity reduces under the influence of shear, ultimately due to the no-slip condition on the flat wall surface. This reduction in streamwise momentum allows the fluid to be more easily turned under the influence of the cross flow pressure gradient. In this way, flow is "overturned" near the flat wall such that low momentum fluid congregates in the corner made by the flat and convex walls.

This generic description represents the flow field existing in axial compressor endwalls, as illustrated in Fig. 1. From a compressor performance standpoint, 3-D boundary layer separation at the endwall can have a great effect on flow blockage resulting in a limitation of achievable static pressure rise, limited stable operating range, and reduced efficiency.[1]

Due to the strong link between compressor performance and endwall behavior, ongoing research has focused on improving the understanding of the fluid mechanics in this region. Joslyn and Dring[2] found corner stall in the

---

* Aerospace Engineer, AFRL/RZTF, AIAA Member.
† 1LT, USAF, Aeronautical Developmental Engineer, AFRL/RZTF, non-member.
‡ CARL Director, AFRL/RZTF, AIAA Associate Fellow.

second stage of a multistage research compressor resulted in high aerodynamic loss. At a near stall operating condition, reversed flow was found to 75% of the span. Dong et al.[3] found stall in both stator endwalls, but not in the rotor hub. Schulz and Gallus[4] found corner stall for all conditions tested and that secondary flow was responsible for the generation of high loss in the corner region.

Numerical simulations have also been used extensively to study the flow behavior in the suction side/endwall corner. Hah and Loellbach[5] found that the dominant features of the hub corner flow field at a particular operating condition were two vortices on the hub surface that extended through the local boundary layer into the main flow and, in fact, were ends of the same vortex. One end of the vortex was associated with separation as the flow lifted off the surface while the other end was associated with reattachment. They concluded that corner stall is caused by a three-dimensional vortex system which does not correlate with the classical Lieblein[6] Diffusion Factor design parameter. Gbadebo et al.[1] examined the behavior of compressor vane corner flow field as computed by RANS (Reynolds Averaged Navier-Stokes) simulation and its correlation to surface flow visualization results. They concluded that for a blade/endwall corner with no clearance, separation is universal and the quality of a design hinges on the thickness of the separation. Further, they claim that since the size of the separated region is sensitive to the turbulent entrainment process at the boundary layer edge, RANS methods will be subject to error due to limitations in the accuracy of turbulence modeling.

Lei et al.[7] developed a criterion to determine whether hub corner stall exists in a passage based on parameters readily available during the preliminary design process. The authors state that “the principal three-dimensional effect is the secondary flow, due to the cross passage pressure gradient, which brings low stagnation pressure, low momentum fluid into the hub corner region.” Three basic processes found to govern the formation of hub corner stall were: 1) the adverse pressure gradient in the blade passage, 2) the cross-flow from pressure to suction side due to the overturning of the fluid near the endwall inside the blade passage which brings low momentum fluid to the hub corner region, and 3) the condition and skew of the incoming endwall boundary layer flow which affects the strength of the cross-flow and the resistance to reversal. The three processes are illustrated in Fig. 1.

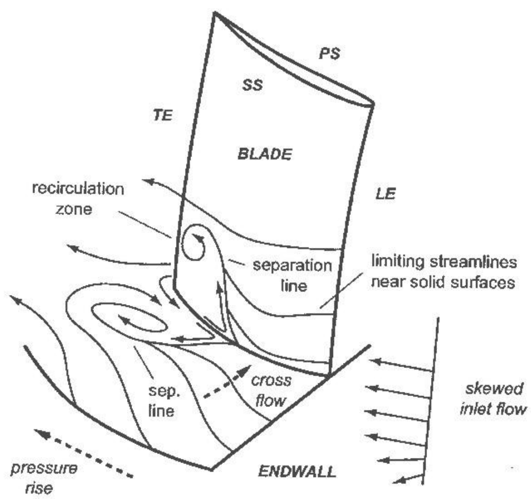

Figure 1. Compressor blade endwall flow field illustrating the flow processes that govern the formation of hub corner stall (Lei et al.[7]).

Attempts at controlling the stalled corner flow field were reported as early as Peacock[8] and Stratford.[9] Gümmer et al.[10] explored the synergistic benefit of employing customer bleed slots in the proper location in the stator passage to significantly reduce corner stall. The authors found that a powerful tool in controlling corner stall lay in intercepting the cross flow, low momentum boundary layer fluid before it reaches the corner and interacts with the blade boundary layer and in concert blooms into full separation under the influence of the adverse streamwise pressure gradient. An interesting observation from this work is that indiscriminate use of flow suction can actually make the corner stall worse. The implication is that the flow in the corner regions of the blade passage is very nearly separated, if not actually separated, during typical operation. By removing flow at a position where the boundary layer is “healthy”, the passage is asked to increase diffusion. When that occurs, the low momentum fluid in the endwalls becomes fully separated or the already separated region in the endwalls becomes even larger. Both are associated with increased blockage and loss. Therefore a highly loaded passage will not benefit from blade surface flow control alone, where most previous studies have concentrated. In order to investigate the efficacy of their corner stall criterion, Lei et al.[7] employed a flow control approach where flow was injected downward on the suction side of the airfoil to produce an opposition to the cross-passage low momentum flow. The result was elimination of the endwall-surface separation, but separation on the blade surface remained. Injection of 0.8% of the main flow was found to reduce the overall loss coefficient by about 10%.

Most recently, research involving flow control on stator vanes has underscored the need to address flow separation occurring in the blade suction side/endwall corner. Culley et al.[11] investigated stator suction surface-mounted slots and jets in a low speed, multistage research compressor using steady and unsteady blowing. Two vanes were modified in the stator ring to use the flow control approaches and measured in detail. They estimated an overall reduction of 25% area-averaged loss while injecting 1% of the compressor throughflow. While a reduction in loss coefficient was observed over most of the span, they concluded that a separate endwall flow control approach was necessary to achieve any significant reduction in the high losses at the problematic stator-hub corner. Kirtley et al.[12] investigated steady blowing on the suction surface in a full stator ring in a low speed, multistage research compressor where the loading of the stator was increased significantly. One percent of the overall compressor mass flow was used to reattach the stator suction surface boundary layer. Of interest to the current work is the observation that the suction side flow control was unable to fully "repair" the separated boundary layer flow where large secondary flows and high endwall loading predominate. They found, in fact, that when the flow control was turned on, the endwall loading went up and increased separation. Car et al.[13] and Bailie et al.[14] demonstrated a reduction in separation in the endwalls of a curved, diffusing passage with very high loading through the use of two different configurations of slot jets. Five percent or more injection flow was used in a slot jet with vortex generators and a slot jet with a tailored profile in the streamwise direction, which resulted in a significant increase of total pressure near the endwalls.

In summary, endwall flow behavior is generally quite complex, and it significantly influences compressor performance. The primary factors that influence the existence and extent of three dimensional boundary layer separation in the convex surface/endwall corner are pressure rise through the passage, cross-stream secondary flow resulting from the interaction between the cross passage pressure gradient and the endwall boundary layer, and the state of the incoming boundary layer. Flow control applied to the corner separation problem has thus far focused primarily on disrupting the secondary flow using flow removal techniques. Exceptions to these efforts are those of Lei et al.[7] and Car et al.[13] where momentum injection has been used. None of the flow control efforts to date have been able to maintain fully-attached boundary layers on both the endwall and the blade surface at loading and efficiency levels required by current and future compression systems.

II. Technical Objective

The ultimate intent of this work-in-progress is to investigate the potential of active and passive flow control means to improve compressor stator performance. Toward that end, it was first necessary to investigate the three dimensional separation characteristics, associated losses and near surface streamline topology typical of a state-of-the-art core compressor stator at typical on- and off-design operating conditions. This "baselining" phase is the focus of the current paper.

Future work will use findings of the baseline investigation to guide strategic implementation of various flow control approaches for loss reduction and/or off-design range extension. The early phases of the research program rely on high-fidelity CFD to sufficiently characterize the stator endwall flowfield and conduct topological sensitivity analysis with flow control. It is planned that approaches showing significant promise in the simulations will then be evaluated experimentally in an annular cascade facility.

III. Approach

A stator vane has been designed typical of the inlet stage of a multistage core compressor of moderately high loading. The philosophy used during the design was to achieve the best aerodynamic performance while avoiding the use of three dimensional blade shaping techniques such as bowing and end bends. This was thought to provide a more generic baseline for evaluation of the basic three dimensional boundary layer separation challenges that could subsequently be addressed separately by flow control and 3d design approaches in a competitive fashion.

Numerical simulations of the baseline configuration have been performed. These provide high resolution flow field data, such as the pressure field and detailed vortical structures in the corner separation, where measurements cannot be obtained or are difficult to obtain. This is particularly important considering the complexity of the flow structures inherent to corner separations[1,5]. The commercial, unstructured RANS solver *FLUENT* has been employed, since it offers a wealth of solver and turbulence modeling options, and can support grids of complex geometries, including flow control features, in full detail.

IV. Design Methodology

A preliminary design of a multistage machine with relevant overall performance parameters was accomplished utilizing an in-house developed meanline design program. A constant radius meanline configuration was used. The inlet stage was to be the focus of the current effort and its design parameters are given in Table 1.

Table 1. Inlet stage meanline design parameters.

	Rotor	Stator
Pressure Ratio	1.935	1.918 (stage)
Inlet Corrected Specific Flow Rate	36.36 lbm/s/ft^2	30.12 lbm/s/ft^2
Corrected Meanline Blade Speed	1183 ft/s	0 ft/s
Meanline Relative Mach Number	1.21	0.72
Meanline Axial Velocity Ratio	0.98	0.96
Meanline Diffusion Factor	0.51	0.51
Meanline Solidity	1.9	2.1
Aspect Ratio	1.1	0.9
Reaction	n/a	0.745 (stage)

The streamline curvature throughflow program *UD0300* was used to do the detailed design and create the blade shape. The meridional view of the inlet stage, with focus on the stator, is provided in Fig. 2.

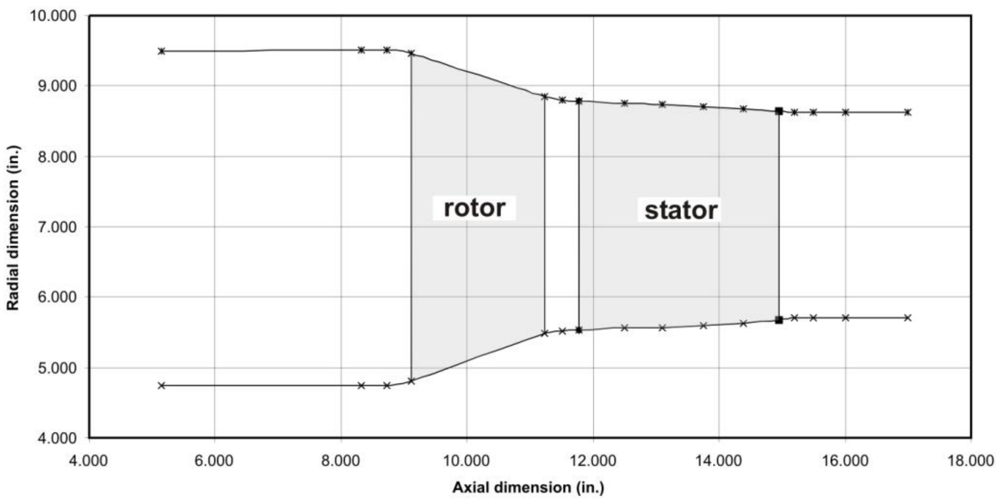

Figure 2. Meridional view of flow path used for stator design in the throughflow design program.

Since current interest is focused on the stator, the rotor was not designed in detail. It was simply represented geometrically by its blade edges (no internal definition) along with a constant spanwise work distribution. The stator was represented by its leading and trailing edge computing stations along with 4 internal stations. The design therefore incorporated “arbitrary airfoils” rather than that of a given airfoil family. This provided the designer with control of the stator’s streamwise loading distribution, where 70% of the diffusion was allocated to the front half of the blade passage.

The blade thickness distribution was defined by analytical expressions where blade edge thickness and magnitude and position of max thickness were specified. For this design, the blade edges varied from 0.4 to 0.5% of chord, the max thickness varied from 4% (hub) to 6% (tip) of chord, and the position of maximum thickness was a constant 55% of chord over the span. A constant 3 degrees incidence angle was specified and Carter’s Rule was used to calculate the deviation angle with a constant 1 degree added. The resulting airfoil is shown in Fig. 3.

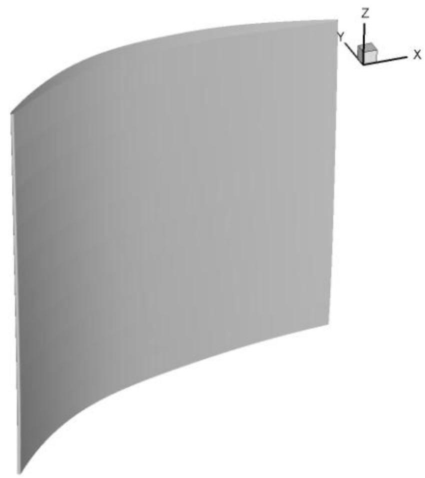

Figure 3. Stator airfoil designed for the current study.

V. Computational Methodology

The focus of this study is a highly-loaded core compressor stator bladerow, with the baseline design generated by meanline and throughflow analysis. The computational domain of interest is the single annular bladerow, which consists of 28 stator vanes fixed at both the hub and tip. As shown in Fig. 4, periodic boundaries are employed so that only a single stator passage has to be modeled. To reduce numerical error in the critical leading edge (LE) region, a vane-centered arrangement is used. Hub and tip fillets are not presently modeled. The domain extends axially one chordlength up- and down-stream of the airfoil leading and trailing edges, respectively.

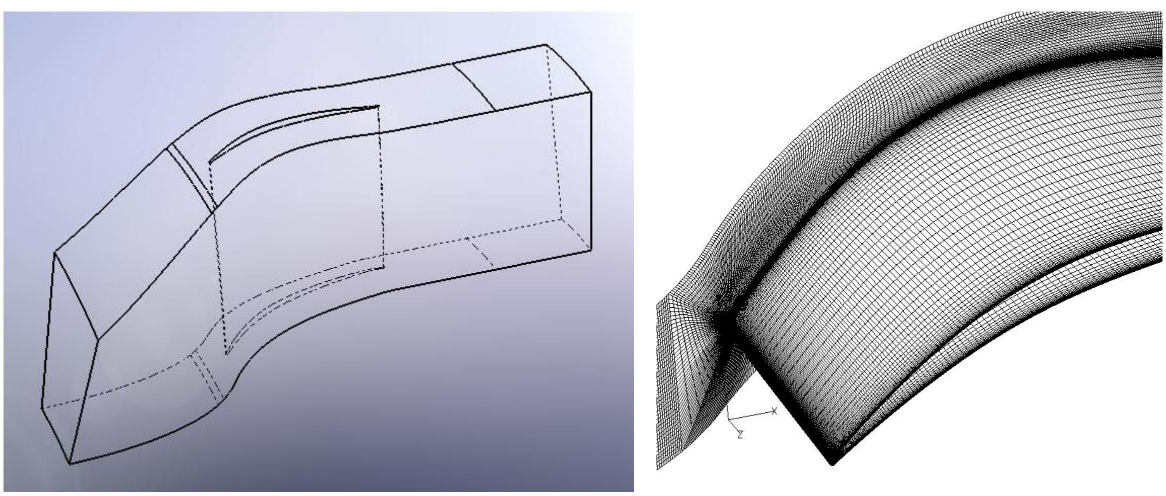

Figure 4. Computational domain (L) and surface grid (R) for baseline stator airfoil.

A very high-density multi-block mesh consisting of 2.14 million hexahedral cells was generated for the single blade passage using *Gridgen*. A surface-fitted O-grid was used to minimize cell skewness near the airfoil surface. This was nested within another O-grid which extended in the pitchwise direction to the periodic boundaries and in the axial direction to constant axial stations. H-meshes were then used to extend the domain axially, both up- and downstream. Cells were tightly packed at all solid boundaries to fully resolve boundary layers and 3d separation. A view of the hub and airfoil surface grid near the leading edge is provided in Fig. 4.

Boundary conditions were specified as follows. Total pressure and total temperature were specified at the inlet based on the stator design radial profiles, given in Fig. 5, which represent the outflow from the notional rotor. Similarly, the inlet flow angle (swirl) was specified for the design incidence (+3°) and varied uniformly for the off-design incidence cases (-1, +1, +5°). Exit static pressure was specified and adjusted for all cases to maintain the same mass-averaged inlet Mach number (0.72) as the design condition. Periodic boundaries were specified in the circumferential direction. The remaining solid boundaries were modeled as no-slip without wall functions.

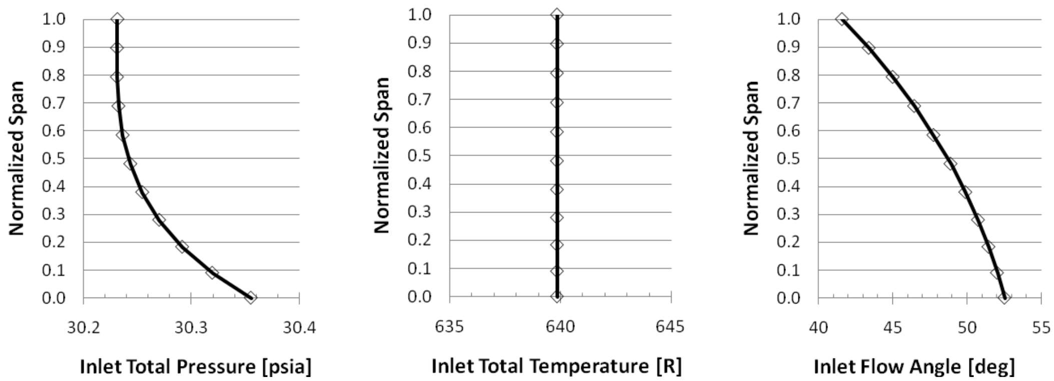

Figure 5. Prescribed stator inlet boundary conditions based on notional rotor exit flow.

Except where otherwise noted, the following computational scheme was used. The Reynolds averaged Navier-Stokes (RANS) equations were solved using *FLUENT*'s parallel, steady, 3d, pressure-based, implicit solver. Turbulence closure was approximated with the *k-omega* model with Shear Stress Transport (SST-kω), with compressibility effects included. The simulations were typically run with 24 processors on the SGI Altix 4700 cluster at the Air Force Research Laboratory's Major Shared Resource Center (AFRL MSRC). Steady or declining residuals below 1e-4 for continuity and 1e-5 for momentum were taken to be indicative of solution convergence.

VI. Results

The following section describes initial results from the on-going research program. Performance and flow behavior are described at the design condition as well as off-design conditions. Off-design parameters considered are varying incidence angle and inlet Mach number.

A. Design Flow Conditions

Flow through the stator passage was first simulated at the design conditions, including a mass-averaged inlet Mach of 0.72 and the design inlet swirl distribution (ref. Fig. 5). Figure 6 provides a comparison of the inlet conditions from the throughflow design with those of the CFD simulation (at design incidence). Shown are radial distributions of total pressure, flow angle (swirl) and absolute Mach number. Since the CFD flow domain extends significantly upstream of the stator leading edge (LE), the CFD values are taken from within the flow domain, at an axial station just upstream of the LE. The presented values represent circumferential averages.

It is evident that the total pressure profile is closely matched to the throughflow design intent, which is expected since this is a specified boundary condition. The agreement between the flow angle and Mach profiles is deemed acceptable, though there is some variation from the design intent. Specifically, the simulation flow angle at the hub is approximately 1 degree lower than the design intent. This still represents a positive incidence angle, since the throughflow design intent is for constant spanwise incidence of +3°. The Mach distribution deviates some in the mid-span, likely due to the blockage effects of the endwall boundary layers (BL) in the simulation. Nonetheless, the mass-averaged inlet Mach values are closely matched.

These results demonstrate that the basic design intent of the incoming flowfield has been modeled acceptably. The overall performance and internal flow physics of the stator passage at design flow conditions will be discussed in more detail in the following sections, as comparisons are made to the off-design flow conditions.

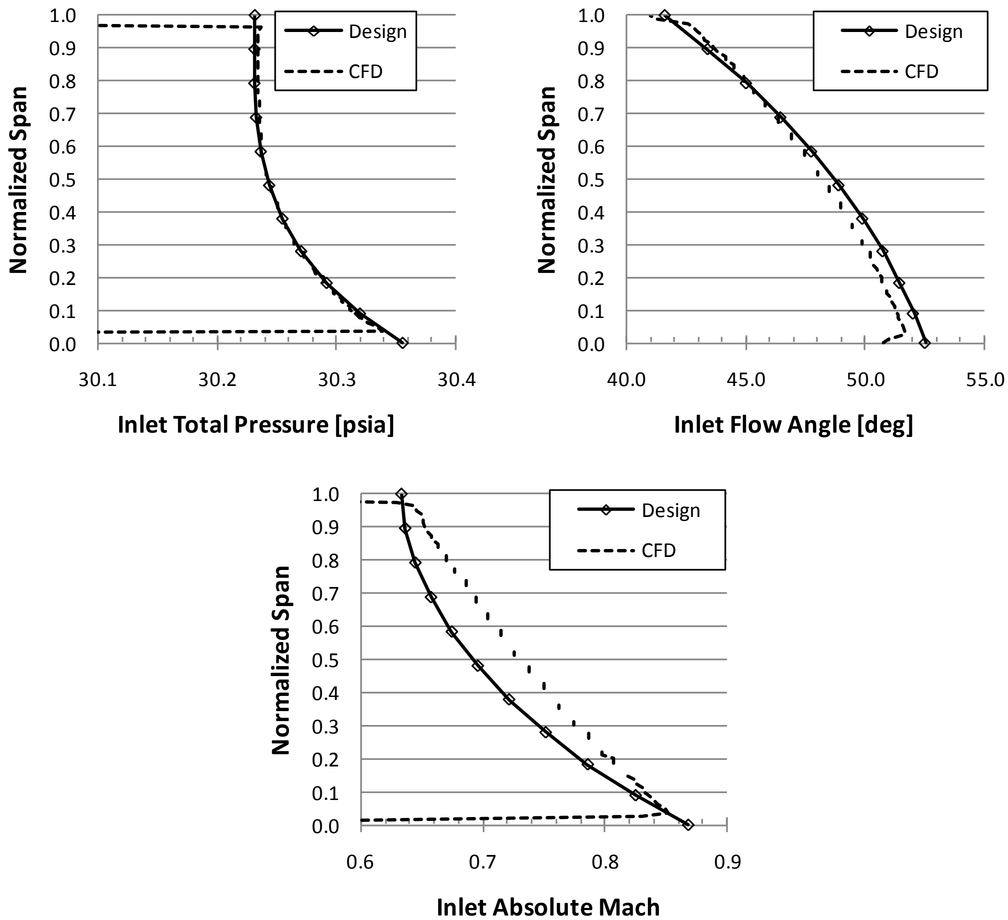

Figure 6. Comparison of throughflow design values with circumferential averages of the computed radial inlet profiles, interrogated just upstream of the stator leading edge.

B. Incidence Angle Effects

A primary goal of the baselining phase is to assess the effect of varying incidence angle on the flow behavior and overall performance of the stator. As is typical practice for evaluating loss characteristics in turbomachinery cascades, the varying incidence cases are compared at equivalent inlet Mach number conditions. Since the inlet Mach profile could vary slightly from case to case, it was deemed most appropriate to match the mass-averaged inlet Mach number ($M_{ma,in}$) at the design value, $M_{ma,in}$=0.72.

To evaluate the flow features internal to the stator passage, surface oil flow and vortex core visualization was generated using the *FieldView* CFD post-processing software. Figure 7 provides flow visualization images from steady solutions at four different incidence conditions, ranging from -1° to +5°. Three periodic stator passages are shown, with the stator vane removed from the outer two passages for an unobstructed view of the endwall region. The left column provides a view of the stator pressure surface (PS) and the tip endwall surface. The view in the right column is of the stator suction surface (SS) and the hub endwall surface. In both views the predominant flow direction is from left-to-right. The surface-restricted oil flow visualization of the so-called “limiting streamlines” is shown in blue, while the approximate vortex cores extracted by *FieldView*’s vorticity alignment method are shown in yellow.

Convergence of a steady solution at the +5° incidence case was found to problematic. Unsteady simulations are underway to resolve periodic unsteady behavior and enable time-averaging. For comparison purposes, a case using the Spalart-Allmaras (S-A) one-equation turbulence model, which more nearly achieved steady convergence than the SST-kω case, is included at present in Fig. 7.

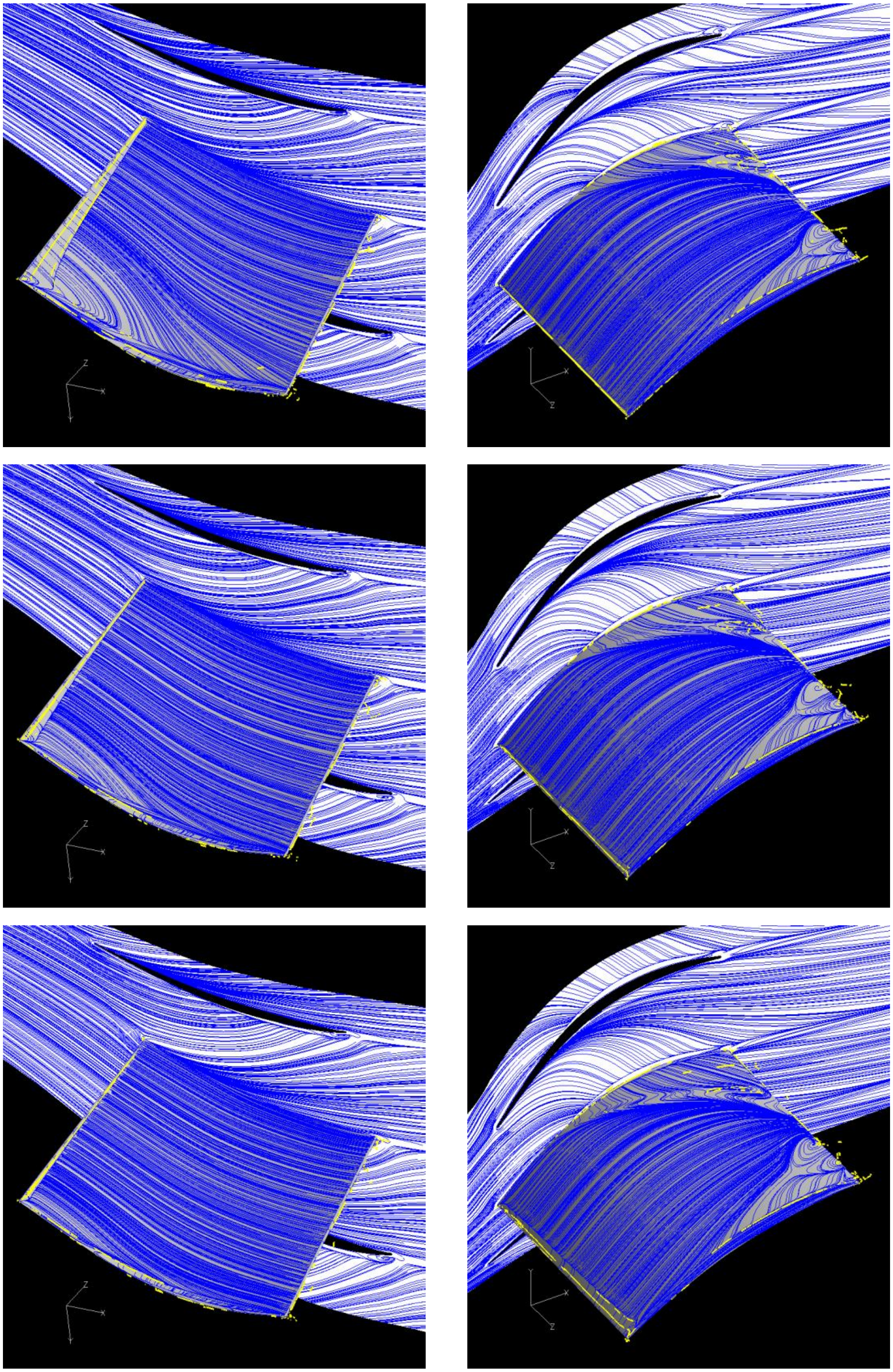

(a) -1°

(b) +1°

(c) +3°

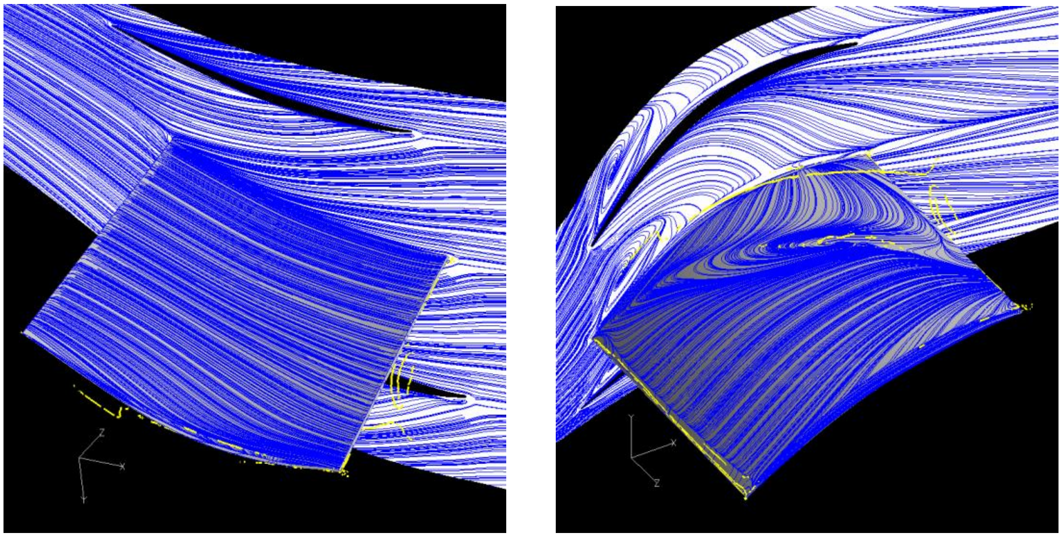

(d) +5°

Figure 7. Oil flow and vortex core visualization on stator and hub surfaces at $M_{ma,in}$=0.72 for varying incidence angles, as noted. The S-A model is shown for +5° instead of SST-kω.

All of the cases in Fig. 7 show a region of bound vorticity at the stator LE which, consistent with the oil flow visualization, indicates a small separation bubble. At reduced incidence angles the separation appears on the PS, whereas for design and higher incidence the LE separation appears on the SS. To varying degrees, small LE shocks were detected and are consistent with the separation location. The small region of supersonic flow stems from highly localized flow acceleration around the circular LE. It is noted that some turbine engine manufacturers insist on elliptical LE shapes for this and perhaps other reasons. It is physically plausible that the high subsonic inlet Mach numbers can indeed result in the observed shocks, especially at the hub. However, an evaluation is underway to determine whether grid skewness near the LE may have caused some numerical exaggeration of this tendency. Nonetheless, in all cases the separated LE flow is seen to reattach quickly without any obvious impact on the development of the downstream flow features.

Flow along the PS and tip endwall (left column) is generally noted to be well-behaved and consistent for all incidence angles, with one exception. For the negative incidence case, oil flow on the PS indicates some secondary (non-streamwise) flow behavior with limited recirculation near the LE-hub corner. This effect is seen to disappear with increasing incidence angle.

For all cases, the SS and hub endwall flow are seen to be complex, with three-dimensional separation clearly indicated at both hub and tip. Very similar to findings reported by other authors cited in this paper, the present separation zones are noted by complex flow patterns on the SS, with endwall separation lines bounding what appears to be a thin separated zone in the pitchwise direction. The SS flow topology is very similar for all but the highest incidence case. At +5° a full hub-corner stall is noted, beginning near the LE, with a coherent vortex core emanating from the hub surface near the LE. The hub-corner flow appears to be the source of the unsteady effects which limit steady solution convergence for this case. The SS oil flow indicates a much stronger flow recirculation from the TE towards the LE than the lower incidence cases. There is also increased spanwise extent of the hub-corner separation, with sufficient blockage to locally accelerate (and thereby improve) the stalled tip-corner flow.

It is noteworthy that the observed large hub corner stall at +5° incidence was not expected according to the criterion established by Lei et al.[7] They used incompressible CFD analysis to document a wide range of compressor cascade configurations (both rotors and stators), and were able to effectively collapse the data with a "hub-corner stall indicator" and a "diffusion parameter". The diffusion parameter is similar to that of Lieblein (1959), but is defined purely based on geometric details, including a term for skewing of the incoming boundary layer. Lei found that hub-corner stall was clearly indicated above a critical value of 0.4 (+/- 0.05) for the diffusion parameter. The reader is directed to Lei et al.[7] for more detail.

The present case in question has diffusion parameters (per Lei's definition) of 0.24, 0.25 and 0.21 at the hub, mid and tip sections, respectively. These are well below the critical value suggested by Lei, but further analysis is necessary to rule out potential numerical artifacts associated with the grid quality and the lack of full steady convergence at +5°, which will be difficult to obtain if the corner stall remains. Perhaps more importantly, any compressibility and shock-related effects are certainly beyond the scope of Lei's formulation.

Overall aerodynamic performance of the stator blade row, provided in Fig. 8, is based on mass-averaged quantities at the inlet and exit plane. The diffusion factor (DF) is that of Lieblein,[6] while the total pressure loss coefficient (ω) and static pressure rise (C_{SPR}) coefficient are formulated as follows:

$$\omega = (Pt_{in} - Pt_{out}) / (Pt_{in} - Ps_{in}) \tag{1}$$

$$C_{SPR} = (Ps_{out} - Ps_{in}) / (Pt_{in} - Ps_{in}) \tag{2}$$

where Pt and Ps represent the total and static pressure, respectively, and subscripts *in* and *out* denote the inlet and exit stations.

Total pressure losses between -1° to +3° incidence are acceptably low, ranging from 5.6 to 6.2%, and this despite the presence of 3-D corner separation (ref. Fig. 7). The reader is reminded of the finding of Gbadebo et al.[1] that such corner separation occurs universally, though it is typically thin with acceptably low blockage penalty. Static pressure rise coefficient and diffusion factor both increase steadily with increasing incidence up to the +3° design value.

At +5° incidence, the loss coefficient jumps harshly, almost three-fold, while the pressure rise falls sharply. These indicators of poor performance are clearly consistent with the observation of the large hub-corner stall at high incidence. Despite the dramatic changes in the pressure performance metrics, the computed diffusion factor does not drop substantially. This demonstrates that the typical DF formulation, though an effective and widely used preliminary design tool, is not a good indicator of far off-design (e.g. post-stall) performance.

While the fall-off in performance at increased incidence is undesirable from a design standpoint, it is not unexpected. A designer might now choose to make some geometric adjustments to extend the stall boundary and/or reduce the losses of the stator. However, the baseline stator appears to be meet the basic design intent and is well-suited for the planned flow control sensitivity study for the following reasons: (1) 3d separation is present; (2) losses are typical, but not insignificant, near design incidence; (3) losses increase greatly and the separation topology changes dramatically at increased incidence. Moreover, there is certainly margin for improvement through 3d shaping design techniques. Thus the authors' intent to evaluate both conventional geometric and flow control approaches in a competitive fashion is supported.

C. Mach Number Effects

Since hub-corner stall and related unsteady effects were noted at +5°, and considering the possible role LE shocks might play in these effects, it was decided to evaluate the effect of reduced inlet Mach number. This was accomplished by increasing the back pressure boundary condition, while maintaining the inlet total pressure and swirl angle distributions.

Four cases, with mass-averaged inlet Mach varying from the design condition down to 0.21, were run and the overall performance is summarized in Fig. 9. As expected, the total pressure losses decrease for decreasing inlet Mach, and the static pressure rise coefficient correspondingly increases.

Figure 10 provides surface oil flow visualizations for the varying inlet Mach conditions. The two lowest Mach conditions were free of LE shocks, but both still show a small LE separation zone. More interesting is the apparent elimination of the hub-corner stall for the M=0.21 case. A change in the suction surface flow pattern is also evident, such that the M=0.21, +5° case seems to more closely resemble the other incidence cases at high inlet Mach than the high Mach, +5° condition. It is also noteworthy, and likely due to elimination of the corner stall, that steady convergence was most readily achieved for the lowest Mach condition.

Before moving on to the flow control application phase, several tasks remain to complete the baselining work. The stator LE curvature will be modified using an elliptical profile instead of a circular one, and a new grid will be generated with higher resolution and reduced skewness near the LE. These changes are intended to address both physical and numerical factors which may adversely contribute to the predicted LE shock-related effects. In addition, proper time-averaged-unsteady, if not steady, solutions will be obtained for all conditions of interest.

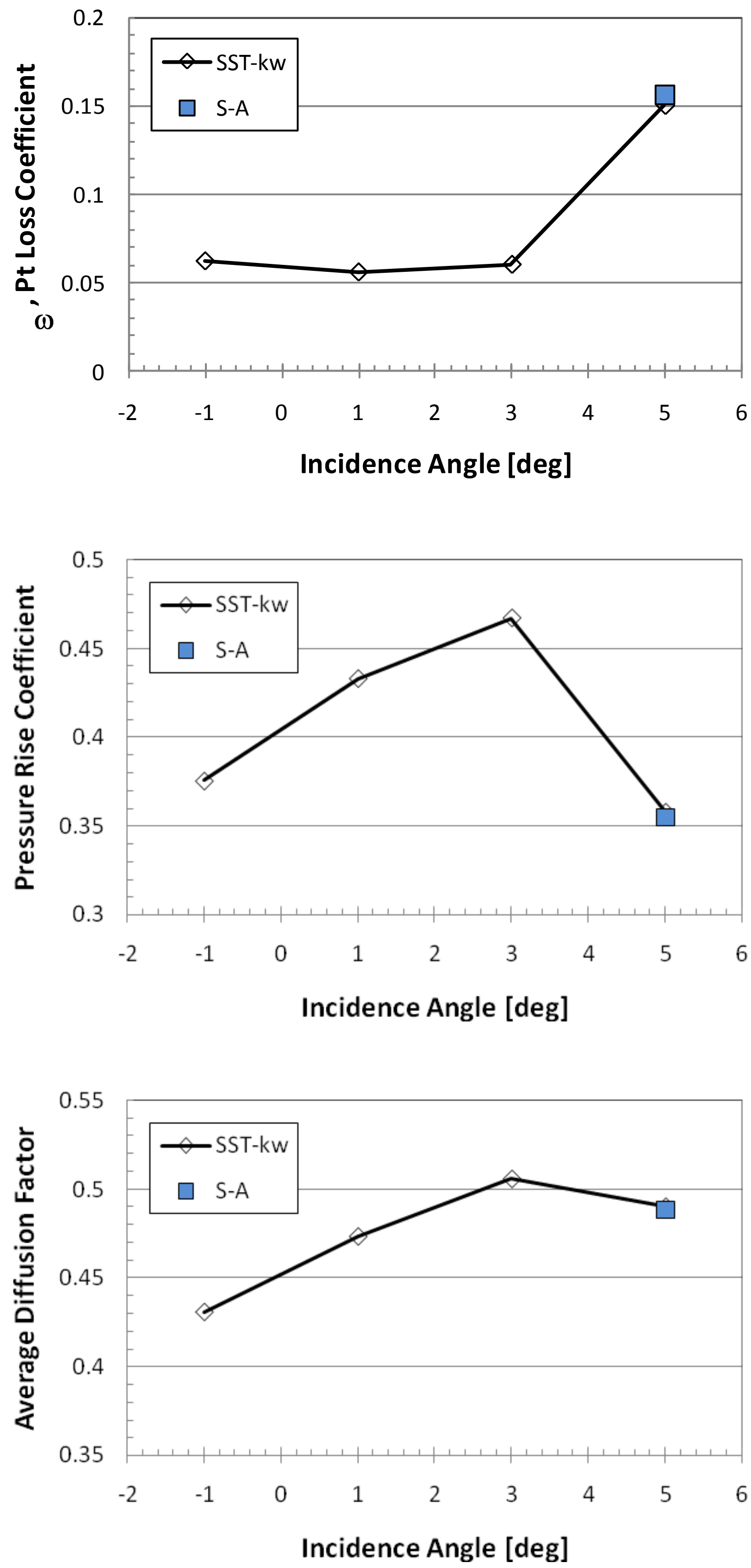

Figure 8. Overall stator performance metrics at $M_{ma,in}$=0.72.

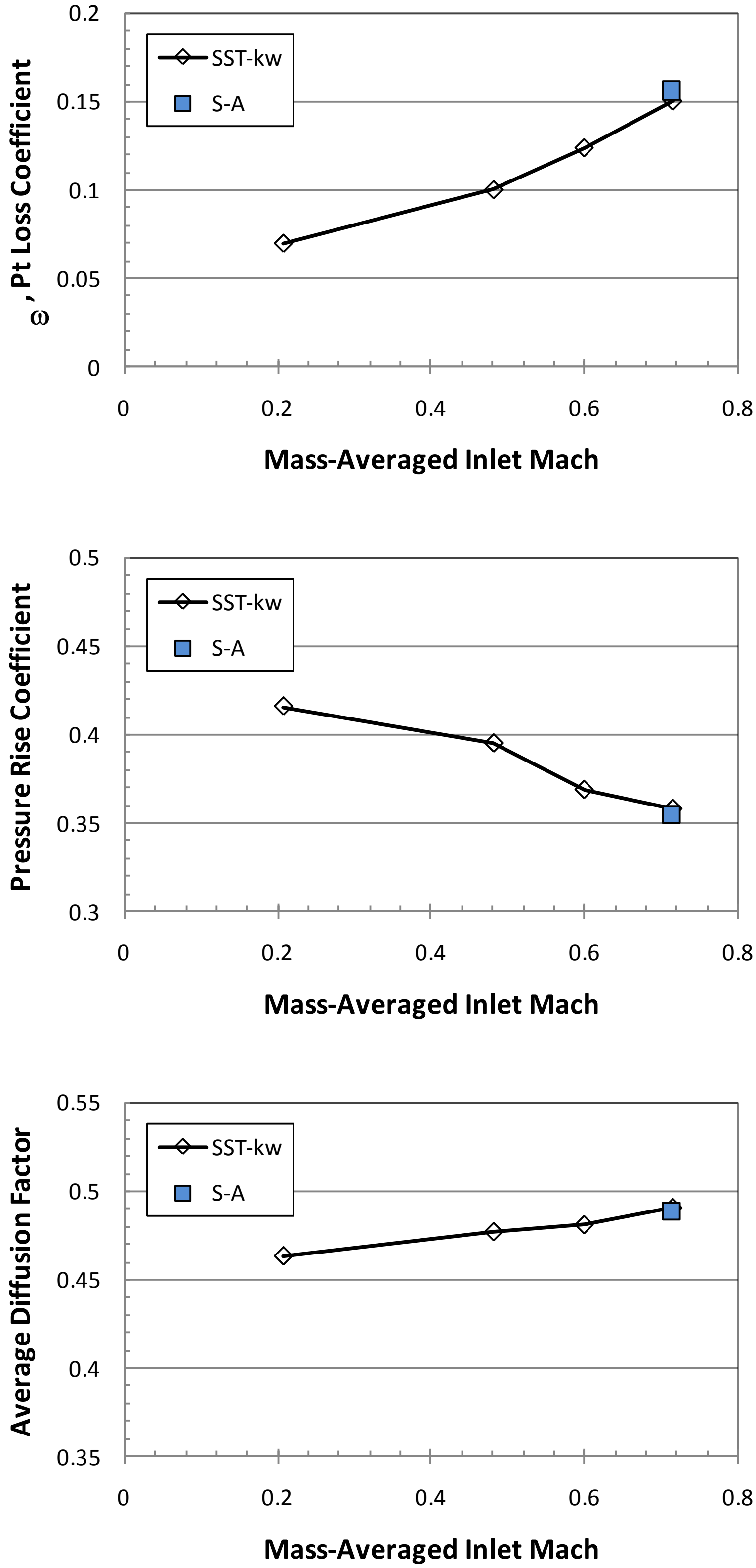

Figure 9. Overall stator performance metrics at incidence of +5°.

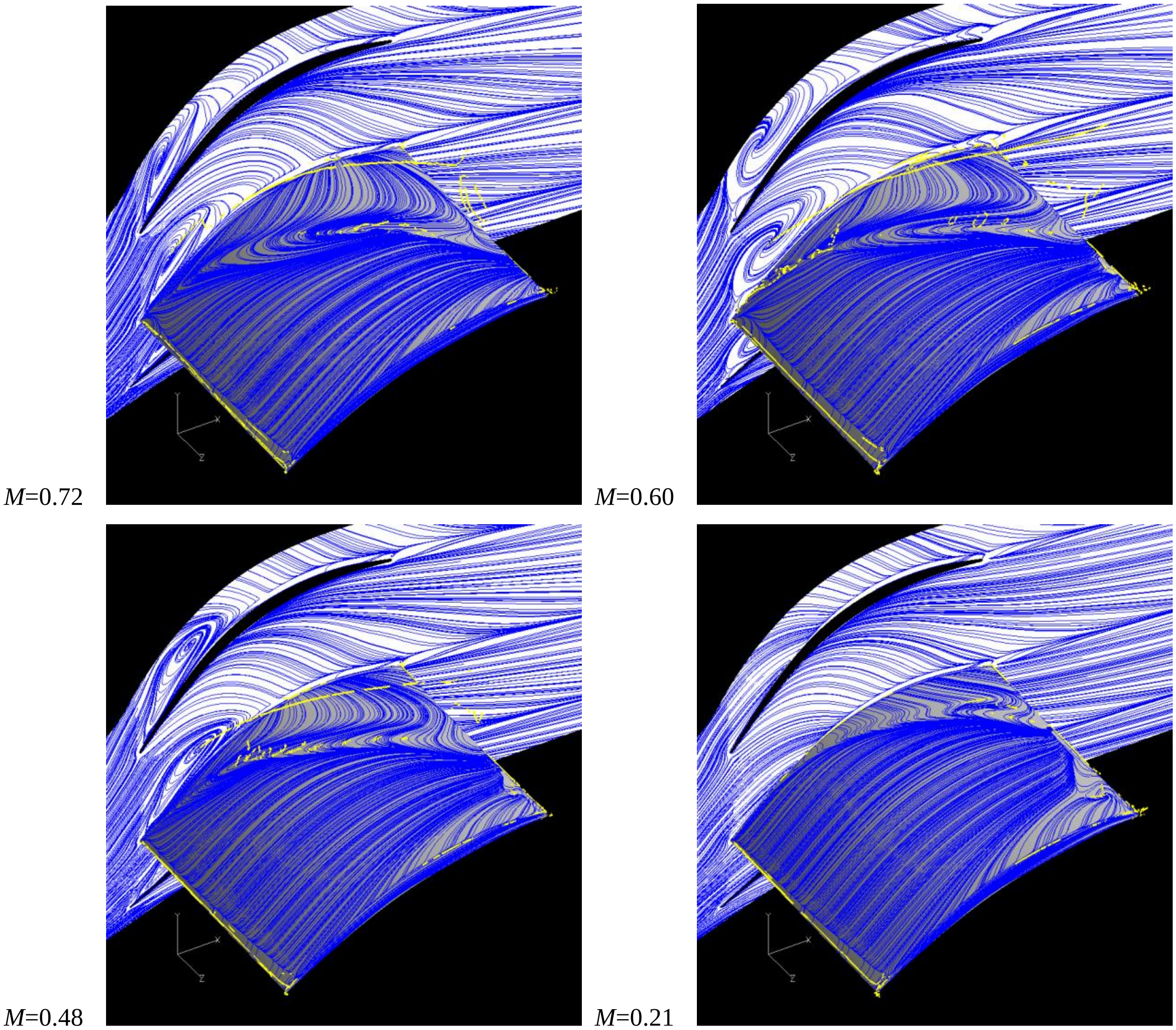

Figure 10. Oil flow and vortex core visualization on hub and stator suction surfaces at +5° incidence for varying inlet Mach, as noted. The S-A model is shown for $M_{ma,in}$ =0.72.

VII. Conclusion

As part of an on-going research program seeking improved aerodynamic performance of highly-loaded compressor stators, a baseline stator has been designed and computationally evaluated. Some observations of the baseline design are included below:

- Despite the presence of small 3-dimensional corner separations, the baseline stator design has typical low loss at design and reduced incidence angles.
- As expected, static pressure rise is best at design incidence and is reduced for off-design incidence.
- At increased incidence (+5°), a large hub-corner stall results in greatly increased total pressure loss and limits the static pressure rise.
- For the subsonic design inlet Mach number distribution (average of 0.72), local acceleration creates a small leading edge shock and separation bubble for all incidence angles simulated. Modifications to LE shape and grid are planned to minimize this tendency.

- Reducing inlet Mach at high incidence reduces losses and eventually eliminates the hub-corner stall.
- The stator appears to be meet basic design intent and is well-suited for the planned flow control sensitivity study for the following reasons: (1) 3d separation is present; (2) losses are typical, but not insignificant, near design incidence; (3) losses increase greatly and the separation topology changes dramatically at increased incidence.

Acknowledgments

The authors gratefully acknowledge the support of Dr. Hugh Thornburg of the AFRL/MSRC for building the grid and for getting the initial simulations off the ground. Thanks are also due to colleagues Mike List, Dave Car and Tom McCray for insightful discussions and timely system support.

References

[1]Gbadebo, S.A., Cumpsty, N.A., and Hynes, T.P., 2005, "Three-Dimensional Separations in Axial Compressors," ASME Journal of Turbomachinery, Vol. 127, pp. 331-339.

[2]Joslyn, H.D., and Dring, R.P., 1985, "Axial Compressor Stator Aerodynamics," ASME Journal of Engineering for Gas Turbines and Power, Vol. 107, pp. 485-493.

[3]Dong, Y., Gallimore, S.J., and Hodson, H.P., 1987, "Three-Dimensional Flow Phenomena in a Transonic, High-Throughflow Compressor Stage," ASME Journal of Turbomachinery, Vol, 109, pp. 354-361.

[4]Schulz, H.D., and Gallus, H.D., 1988, "Experimental Investigation of the Three-Dimensional Flows in an Annular Compressor Cascade," ASME Journal of Turbomachinery, Vol. 100, pp. 467-478.

[5]Hah, C., and Loellbach, J., 1999, "Development of Hub Corner Stall and Its Influence on the Performance of Axial Compressor Blade Rows," ASME Journal of Turbomachinery, Vol. 121, pp. 67-77.

[6]Lieblein, S., 1959, "Loss and Stall Analysis of Compressor Cascades," Journal of Basic Engineering, pp. 387-400.

[7]Lei, V-M., Spakovszky, Z.S., and Greitzer, E.M., 2006, "A Criterion for Axial Compressor Hub-Corner Stall," Proceedings of the ASME Turbo Expo, Paper No. GT2006-91332.

[8]Peacock, R., 1965, "Boundary Layer Suction to Eliminate Corner Separation in Cascades of Airfoils," Tech. Rep., Reports and Memoranda, No. 3663, Engineering Department, University of Cambridge.

[9]Stratford, B., 1973, "The Prevention of Separation and Flow Reversal in the Corners of Compressor Blade Cascades," Aeronautical Journal, pp. 249-256.

[10]Gümmer, V., Goller, M., and Swoboda, M., 2005, "Numerical Investigations of Endwall Boundary Layer Removal on Highly Loaded Axial Compressor Blade Rows," Proceedings of the ASME Turbo Expo, Paper No. GT2005-68699.

[11]Culley, D.E., Bright, M.M., Prahst, P.S., and Strazisar, A.J., 2004, "Active Flow Separation Control of a Stator Vane Using Embedded Injection in a Multistage Compressor Experiment," ASME Journal of Turbomachinery, Vol. 126, pp. 24-34.

[12]Kirtley, K.R., Graziosi, P., Wood, P., Beacher, B., and Shin, H.-W., 2005, "Design and Test of an Ultralow Solidity Flow-Controlled Compressor Stator," ASME Journal of Turbomachinery, Vol. 127, pp. 689-698.

[13]Car, D., Bailie, S.T., and Estevadeordal, J., 2006b, "Slot Jet Flow Control for Diffusion Enhancement: Endwall Observations and Improvements," AIAA Flow Control Conference, Paper No. AIAA-2006-3496.

[14]Bailie, S.T., Car. D., and Estevadeordal, J., 2006, "Streamwise Vorticity Effects in a Curve Diffuser with Slot Jet Flow Control," AIAA Flow Control Conference, Paper No. AIAA-2006-3497.